Proc. Natl. Acad. Sci. USA
Vol. 93, pp. 4925–4930, May 1996
Biochemistry

Translational regulation of mammalian and *Drosophila* citric acid cycle enzymes via iron-responsive elements

(aconitase/energy metabolism/iron regulatory protein/oxidative stress/succinate dehydrogenase)

NICOLA K. GRAY*, KOSTAS PANTOPOULOS*, THOMAS DANDEKAR*, BRIAN A. C. ACKRELL†, AND MATTHIAS W. HENTZE*‡

*Gene Expression Programme, European Molecular Biology Laboratory, Meyerhofstrasse 1, D-69117 Heidelberg, Germany; and †Veterans Administration Medical Center and Department of Biochemistry and Biophysics, University of California, San Francisco, 4150 Clement Street, San Francisco, CA 94121

Communicated by Helmut Beinert, University of Wisconsin, Madison, WI, January 5, 1996 (received for review November 16, 1995)

ABSTRACT **The posttranscriptional control of iron uptake, storage, and utilization by iron-responsive elements (IREs) and iron regulatory proteins (IRPs) provides a molecular framework for the regulation of iron homeostasis in many animals. We have identified and characterized IREs in the mRNAs for two different mitochondrial citric acid cycle enzymes. *Drosophila melanogaster* IRP binds to an IRE in the 5′ untranslated region of the mRNA encoding the iron-sulfur protein (Ip) subunit of succinate dehydrogenase (SDH). This interaction is developmentally regulated during *Drosophila* embryogenesis. In a cell-free translation system, recombinant IRP-1 imposes highly specific translational repression on a reporter mRNA bearing the SDH IRE, and the translation of SDH-Ip mRNA is iron regulated in *D. melanogaster* Schneider cells. In mammals, an IRE was identified in the 5′ untranslated regions of mitochondrial aconitase mRNAs from two species. Recombinant IRP-1 represses aconitase synthesis with similar efficiency as ferritin IRE-controlled translation. The interaction between mammalian IRPs and the aconitase IRE is regulated by iron, nitric oxide, and oxidative stress (H_2O_2), indicating that these three signals can control the expression of mitochondrial aconitase mRNA. Our results identify a regulatory link between energy and iron metabolism in vertebrates and invertebrates, and suggest biological functions for the IRE/IRP regulatory system in addition to the maintenance of iron homeostasis.**

Most animals, including humans and other mammals, frogs, fish, and flies appear to regulate cellular iron metabolism posttranscriptionally by means of the interaction of iron-responsive elements (IREs) and iron regulatory proteins (IRPs) (1, 2). In mammals, where this system is best characterized, IREs regulate the mRNAs for the iron storage protein ferritin, the receptor for cellular iron uptake (transferrin receptor) and the rate limiting enzyme for the main iron utilization pathway, erythroid 5-aminolevulinate synthase (eALAS). By binding to IREs in the 5′ untranslated regions (UTRs) of ferritin and eALAS mRNAs, IRP-1 and, independently, IRP-2 (3, 4) repress the translation of these transcripts (5–9), whereas the transferrin receptor mRNA is stabilized by IRP binding to IREs located in the 3′ UTR (10–12). IRP-1 and IRP-2 bind to IREs in iron deficient, but not in iron replete, cells (3, 13, 14). IRE/IRP interactions thus serve to maintain iron homeostasis by coordinated regulation of iron uptake, storage, and utilization. Moreover, the regulation of IRP-1 by nitric oxide (NO) and H_2O_2 and of IRP-2 by NO (15–19) connects the regulation of iron metabolism to additional signaling pathways (K.P., G. Weiss, and M.W.H., unpublished work).

The publication costs of this article were defrayed in part by page charge payment. This article must therefore be hereby marked "*advertisement*" in accordance with 18 U.S.C. §1734 solely to indicate this fact.

In addition to the mRNAs encoding proteins central to iron metabolism, an IRE motif was identified in the 5′ UTR of porcine mitochondrial aconitase mRNA (20). Like the other citric acid cycle enzymes, aconitase is nuclear-encoded and translated in the cytoplasm. Following their posttranslational import into the mitochondria, the citric acid cycle enzymes form the central pathway for cellular energy metabolism into which amino acid, carbohydrate, and fatty acid metabolism converge. The mitochondrial aconitase IRE motif was shown to bind IRP-1 *in vitro* (21), but the effect of IRP-1 binding on aconitase mRNA expression and its regulation have not been investigated. Since iron and energy metabolism both play critical roles, particularly in proliferating and metabolically highly active cells, we investigated the intriguing possibility of a linkage between iron regulation and the regulation of enzymes of the citric acid cycle. We report that cellular IRPs interact with the aconitase IRE in a specific and regulated fashion. Moreover, we have identified a functional IRE in the mRNA of a second citric acid cycle enzyme, the iron-sulfur protein (Ip) subunit of *Drosophila melanogaster* succinate dehydrogenase (SDH). We show that both IREs function to mediate translational repression by IRP-1.

MATERIALS AND METHODS

Plasmid Construction. All plasmids are derived from pGEM-3Zf(−), and are cloned for transcription from the T7 RNA polymerase promoter. Plasmids hU1A and MSA.CAT have been described (22, 23). Fer.CAT and Mut.CAT contain a wild-type and a mutated ferritin IRE, respectively, upstream of the chloramphenicol acetyltransferase (CAT) open reading frame and have been described as IRE-wt and IRE-mut (9). SDH.CAT was created by ligation of annealed phosphorylated synthetic oligodeoxyribonucleotides into IRE-wt after digestion with *Bam*HI and *Xba*I to remove the ferritin IRE. The sequence of the sense strand oligonucleotide was 5′-GATCTAATTG CAAACGCAGT GCCGTTTCAA TTGT-3′. Acon.IRE was created from pGA (24) that contains the porcine mitochondrial aconitase cDNA lacking 10 nucleotides of the 5′ UTR. The 5′ end of the aconitase cDNA which contains part of the IRE was reconstructed by digestion of pGA with *Bst*EII and partial digestion with *Eco*RI, and subsequent introduction of annealed phosphorylated oligodeoxyribonucleotides. The sequence of the sense strand was 5′-AATTGACCTC ATCTTTGT CA GTGCACAAAA TG-GCGCCTTA CAGCCTACTG-3′. The oligonucleotides used to create Acon.ΔC differ from those used for Acon.IRE by the

Abbreviations: IRE, iron-responsive element; IRP, iron regulatory protein; Ip, iron-sulfur protein; SDH, succinate dehydrogenase; UTR, untranslated region; eALAS, erythroid 5-aminolevulinate synthase; CAT, chloramphenicol acetyltransferase; EMSA, electrophoretic mobility-shift assay; 2-ME, 2-mercaptoethanol.

‡To whom reprint requests should be addressed.

omission of the underlined C in the sequence above. The sequence of all plasmid constructs was confirmed by DNA sequencing.

***In Vitro* Transcription.** Capped mRNAs were generated with T7 RNA polymerase from Fer.CAT, Mut.CAT, SDH.CAT, and hU1A after digestion with *Hin*dIII, and from Acon and Acon.ΔC after *Eco*RI digestion (8). ^{32}P-labeled RNA probes (specific activity ≈3.0 × 10^{7}cpm/μg for the ferritin and SDH-Ip probes and ≈4.5 × 10^{7}cpm/μg for the aconitase probe) and unlabeled competitor RNAs for gel retardation assays were transcribed from Fer.CAT, Mut.CAT, SDH.CAT, and MSA.CAT linearized at *Xba*I, and plasmids Acon and Acon.ΔC linearized with *Bst*EII as described (18, 25). All probes were gel-purified prior to their use.

Cell-Free Translation. Translation-competent extracts were prepared from wheat germ (General Mills) as described (8). Fifteen- microliter cell-free translation reactions were programmed with 2.5 ng of capped *in vitro*-transcribed U1A and 5.0 ng CAT mRNAs, or 20 ng of Acon.IRE or Acon.ΔC mRNAs in the presence or absence of recombinant human IRP-1 purified from *Escherichia coli* as described (8). [^{35}S]methionine-labeled products were analyzed by SDS/PAGE and fluorography (25). All experiments were done at least four times and representative results are shown.

Electrophoretic Mobility-Shift Assays (EMSA). Mouse epidermal JB6 cells were treated as specified in the figure legends, and lysates for EMSA were prepared as described (19). The EMSA was performed in a buffer containing 40 mM Hepes (pH 7.6), 90 mM potassium chloride, 1 mM magnesium acetate, and 2 mM calcium chloride. EMSA using *D. melanogaster* embryo extracts were performed in a buffer containing 22.5 mM Hepes (pH 7.5), 150 mM sodium chloride, 0.25% Triton X-100, 0.1 mM EDTA, and 5% glycerol. Where indicated, 2-mercaptoethanol (2-ME) (2%) was included in the reactions and unlabeled competitor RNAs (60–240 ng) were added prior to the addition of the ^{32}P-labeled probes (3–5 × 10^4 cpm). Heparin (final concentration 5 mg/ml) was added 10 min after the addition of ^{32}P-labeled probes. RNA/protein complex formation was analyzed by nondenaturing gel electrophoresis and autoradiography (26). All experiments were done at least three times with similar results.

Analysis of SDH-Ip Regulation in *D. melanogaster* Schneider Cells. Schneider S2 cells were cultured in Schneider's *Drosophila* medium (GIBCO/BRL)/10% heat-inactivated fetal calf serum (FCS) at 26°C. Following treatment for 10 h with 30 μg/ml ferric ammonium citrate or 100 μM desferrioxamine, cells were either harvested for RNA preparation and Northern blotting (15 μg of total RNA), or labeled for 60 min with 40 μCi [^{35}S]methionine/ml in 2.5 ml of methionine-free Grace's insect cell culture medium (GIBCO/BRL) without FCS as described (15). Cells were lysed in 300 mM NaCl/1% Triton X-100/50 mM Tris·HCl, pH 7.4, and equal quantities of trichloracetic acid-insoluble material (2 × 10^6 cpm) were subjected to immunoprecipitation using saturating quantities of polyclonal rabbit antisera against bovine heart SDH-Ip and protein A-sepharose, and further analysis by SDS/PAGE as described (7).

RESULTS AND DISCUSSION

Conservation of IREs in Mammalian and Invertebrate Citric Acid Cycle Enzyme mRNAs. We previously identified an IRE motif in the 5′ untranslated region of porcine mitochondrial aconitase mRNA (Fig. 1*A*) (20). Using the same IRE search algorithm (27), an identical IRE motif was uncovered in the bovine homologue (Fig. 1*B*), suggesting that this element is conserved among mammals. Strikingly, the search also revealed an IRE-like sequence in the 5′ UTR of the Ip subunit of SDH (Fig. 1*C*), which closely resembles the IRE motif in the two mammalian aconitase mRNAs and matches the "consensus IRE" (Fig. 1*D*) derived from ferritin (Fig. 1*E*) and eALAS (Fig. 1*F*) IREs (20, 28). Two aspects of this observation are particularly noteworthy: (*i*) like aconitase, SDH also participates in the citric acid cycle and (*ii*) this IRE motif is found in the *D. melanogaster* SDH-Ip transcript. If the SDH-Ip and the aconitase IREs were functional, this finding would suggest that IRE-mediated regulation of citric acid cycle enzymes is conserved between mammals and invertebrates.

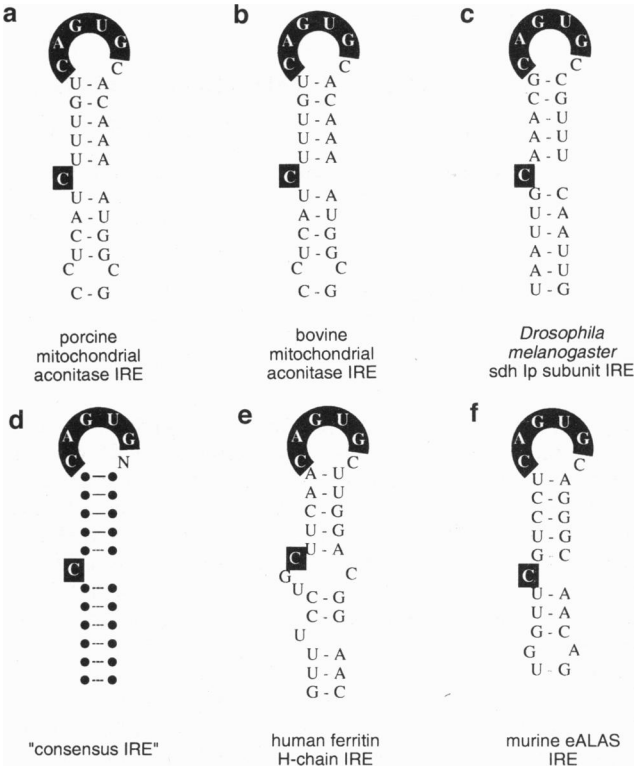

FIG. 1. Identification of IRE motifs in mRNAs encoding citric acid cycle enzymes. The European Molecular Biology Laboratory nucleotide database (including release 44) was screened for IRE motifs using the consensus IRE shown in *D* as described (27). (*A* and *B*) Putative IREs identified in porcine (accession number J05224) and bovine (accession number Z49931) mitochondrial aconitase mRNAs. (*C*) Putative IRE identified within the 5′ UTR of the SDH-Ip mRNA from *D. melanogaster* (accession number L27705). (*E* and *F*) Authentic functional IREs from human ferritin H-chain and murine eALAS mRNAs. The highlighted nucleotides indicate sequence conservation; note the presence of the AUG translation initiation codon in the aconitase mRNA IREs in *A* and *B*).

IRP binding to the SDH-Ip IRE motif was investigated by EMSA. Extracts prepared from 11- to 16-h-old *D. melanogaster* embryos contain a protein(s) that forms a complex with the SDH-Ip IRE probe (Fig. 2*A*, lane 2). Complex formation is reduced in a dose-dependent fashion (60–240 ng) by competition with the human ferritin H-chain IRE (lanes 3–5) and the SDH-Ip element itself (lanes 6–8), but not with the highest concentration (240 ng) of a nonIRE RNA hairpin (lane 9), indicating that both probes form complexes with *Drosophila* IRP. The SDH-Ip IRE competed more strongly than the ferritin IRE, suggesting that the *Drosophila* IRP binds with higher affinity to the *Drosophila* SDH-Ip element. This interpretation is supported by the data shown in lanes 10–18 where the human ferritin IRE was used as a radiolabeled probe. Complex formation is weaker (with the two probes of comparable specific activity, the panel with lanes 10–18 was exposed four times longer), and the unlabeled SDH-Ip element is a stronger specific competitor (lanes 15–17) than the ferritin IRE (lanes 12–14). Conversely, recombinant human IRP-1 forms a stronger complex with the human ferritin than

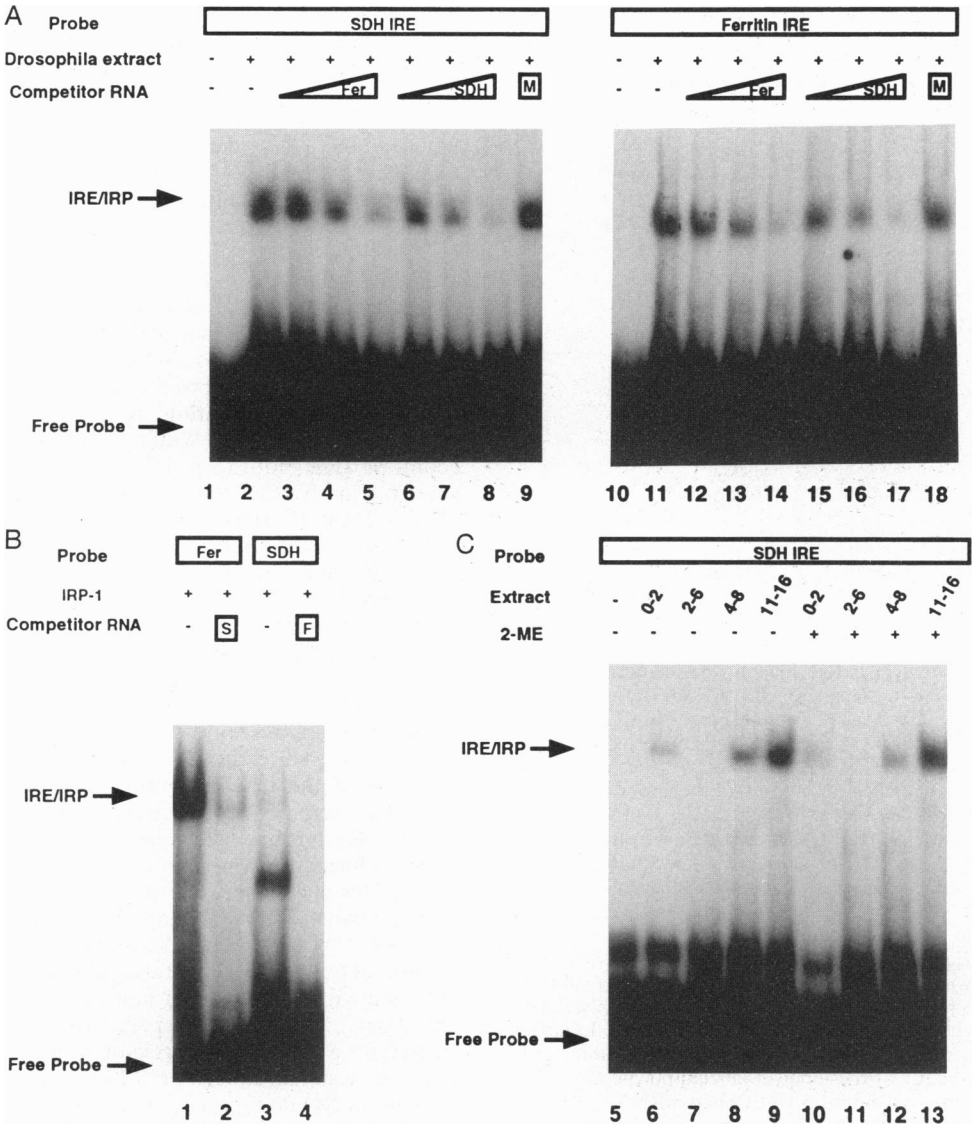

FIG. 2. Binding of IRP to the SDH-Ip IRE is specific and developmentally regulated during *Drosophila* embryogenesis. (*A*) ^{32}P-labeled transcripts containing the SDH.IRE (*left*) or the ferritin IRE (*right*) were incubated with 25 μg of extract prepared from *D. melanogaster* embryos (11 to 16 h after fertilization) and analysed by EMSA. Where indicated, 60 ng, 120 ng, or 240 ng of unlabeled competitor RNAs containing either the ferritin IRE (Fer; lanes 3–5 and 12–14), the SDH.IRE (SDH; lanes 6–8 and 15–17), or 240 ng of a nonIRE related stem loop (MSA) were included (M; lanes 9 and 18). (*B*) Recombinant human IRP-1 (100 ng) purified from *E. coli* (8) was incubated with the ferritin (lanes 1 and 2) or SDH.IRE probe (lanes 3 and 4). Unlabeled SDH (S) or ferritin (F) competitor RNAs (240 ng) were added to the samples in lanes 2 and 4, respectively. The complex with faster mobility in lane 3 may result from a different conformation of the SDH.IRE/human IRP-1 complex than the respective human IRE/human IRP and drosophila IRE/drosophila IRP complexes. (*C*) The SDH.IRE probe was incubated with 25 μg extracts prepared from *D. melanogaster* embryos collected 0 to 2 (lanes 6 and 10), 2 to 6 (lanes 7 and 11), 4 to 8 (lanes 8 and 12), or 11 to 16 (lanes 9 and 13) h after fertilization. 2-ME (2%) was added to the extracts prior to the addition of the probe in lanes 10–13.

the *Drosophila* SDH-Ip probe (Fig. 2*B*, lanes 1 and 3), and the heterologous IREs compete for complex formation (lanes 2 and 4). We conclude that the IRE motif identified in the SDH-Ip mRNA from *D. melanogaster* represents a specific binding site for *Drosophila* and human IRPs. Interestingly, the binding of *Drosophila* IRP to this element is regulated during embryonic development (Fig. 2*C*). While the implications of this developmental regulation have to be investigated further, we note that the modulation of the IRE-binding activity appears to originate from alterations in the total level of IRP [assessed after *in vitro* activation of IRP by 2-ME (29, 30); note the similar binding in lanes 10–13 compared to lanes 6–9] rather than a posttranslational switch between the active and the inactive form of the protein, as has been reported for the regulation of mammalian IRPs in response to NO, H_2O_2, or changes in iron availability (15–17, 19, 31, 32).

Translational Control Mediated by the SDH-Ip IRE. To investigate the regulatory consequences of IRP binding to the SDH-Ip IRE, CAT reporter mRNAs were analyzed. Fer.CAT contains the human ferritin H-chain IRE as a positive control for IRP-mediated regulation, Mut.CAT contains a mutant IRE as a negative control, and SDH.CAT harbors the SDH-Ip IRE. Because the IREs in the SDH-Ip and the ferritin mRNA are located ≈30–40 nucleotides downstream from the transcription start sites [a second SDH-Ip transcription start site 35 nucleotides further upstream has also been identified (33)] and these positions are maintained in the CAT mRNAs (+34 in Fer.CAT and +37 in SDH.CAT, respectively), these indicator mRNAs also suitably reflect a possible regulatory bias inherent in the position of the IRE (34, 35). In the absence of IRP, all three mRNAs are efficiently translated in wheat germ extract (Fig. 3, lanes 2, 5, and 8). Addition of 250 or 500 ng

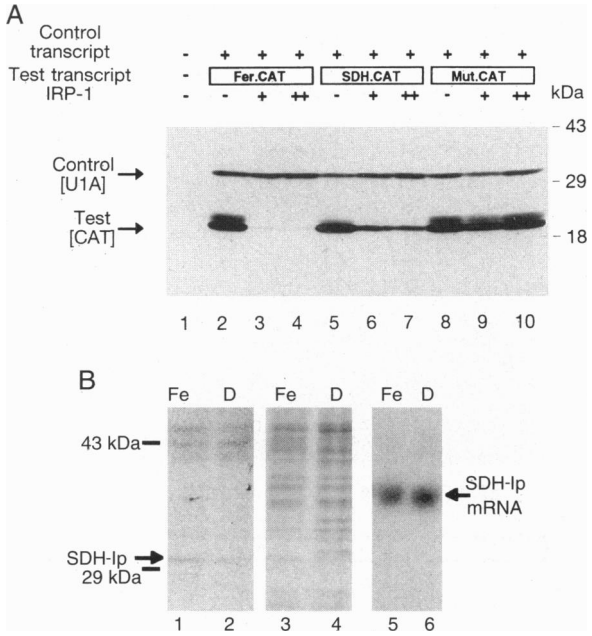

FIG. 3. The *Drosophila* SDH-Ip IRE mediates translational control *in vitro* and in cultured cells. (*A*) Capped U1A mRNA (2.5 ng) (lanes 2–10) was cotranslated with 5 ng of capped Fer.CAT (lanes 2–4), SDH.CAT (lanes 5–7), or Mut.CAT (lanes 8–10) mRNAs in wheat germ extract in the absence (lanes 2, 5, and 8) or presence of 250 ng (lanes 3, 6, and 9), or 500 ng (lanes 4, 7, and 10) of recombinant human IRP-1 purified from *E. coli*. Reactions in lanes 1, 2, 5, and 8 received IRP storage buffer. Molecular weight markers are shown on right and the positions of the U1A and CAT proteins are shown on left. (*B*) *D. melanogaster* Schneider S2 cells were treated with 30 μg/ml of ferric ammonium citrate or 100 μM of desferrioxamine, and analyzed by metabolic labeling and SDH-Ip immunoprecipitation (lanes 1 and 2) or Northern blotting (lanes 5 and 6) as described in the *Materials and Methods*. The identity of the 31-kDa band was confirmed by control immunoprecipitations with protein A-sepharose alone, which yielded the >43-kDa signals, but not the 31-kDa band (not shown). In lanes 3 and 4, equal aliquots of the immunoprecipitation supernatants are shown to assess the equality of the input of labeled polypeptides. In lanes 5 and 6, the position of the ≈1.3-kb SDH-Ip mRNA is shown. Equality of the RNA loading and the electrotransfer was confirmed by the equal staining intensity of rRNAs (not shown).

recombinant human IRP-1 represses CAT synthesis from Fer.CAT and SDH.CAT, but not from Mut.CAT. The specificity of this translational control is further documented by the unaffected translation of the internal control mRNA encoding U1A. In keeping with the stronger binding of human IRP-1 to the ferritin (compared to the SDH-Ip) IRE (Fig. 2*B*), the translational repression of Fer.CAT is quantitatively more pronounced than that of SDH.CAT (compare lanes 3 and 4 with lanes 6 and 7). These results provide direct biochemical evidence for the function of the *D. melanogaster* SDH-Ip IRE as a translational regulatory element. Because the natural position of this element is maintained in SDH.CAT, at least the mRNA originating from the downstream SDH-Ip transcription start site should be regulated by the *Drosophila* IRP. The function of the IRE in the longer *Drosophila* transcript cannot be predicted due to lack of information concerning the functional role of IRE position in invertebrate cells. Interestingly, in the ferritin mRNA from the mosquito *Aedes aegypti* an IRE motif appears to be located at +90 (36), suggesting that in insects IREs may also control translation from more cap-distant sites. To ascertain the function of the SDH-Ip IRE in living cells, *Drosophila* Schneider S2 cells were pretreated with ferric ammonium citrate (Fig. 3*B*, odd numbered lanes) or the iron chelator desferrioxamine (even numbered lanes). Cultures were then analyzed in parallel by metabolic labeling and immunoprecipitation with polyclonal rabbit anti-bovine heart SDH-Ip antisera (lanes 1 and 2), as well as by RNA extraction and Northern blotting with a *Drosophila* SDH-Ip cDNA probe (lanes 5 and 6). In spite of the relatively low affinity of the antiserum raised against bovine SDH-Ip for the *Drosophila* SDH-Ip, the result demonstrates that SDH-Ip synthesis is regulated by changes in iron availability in the absence of alterations in steady-state mRNA levels. Interestingly, analysis of the supernatants reveals the existence of several other polypeptides whose synthesis is regulated by changes in iron availability (lanes 3 and 4). However, with the exception of SDH-Ip, the genetic level of their regulation remains to be defined. We conclude that SDH-Ip expression from the possibly mixed population of SDH-Ip mRNAs is translationally regulated by iron in cultured cells.

Translational Regulation of Mammalian Mitochondrial Aconitase mRNAs. The binding of porcine liver IRP to the aconitase IRE motif (Fig. 1*A*) has been previously reported (21). Curiously, the apo-protein form, the 3Fe-4S and the 4Fe-4S form of IRP-1 were found to bind equally (21), suggesting that the regulation of IRP-1 activity by iron, NO, and H_2O_2 may not be reflected in altered binding to the aconitase IRE. We reexamined this question using lysates prepared from different mammalian cell lines. In extracts from murine JB6 epidermal cells, the aconitase IRE forms a specific complex with IRP-1, as evidenced by the complete competition of unlabeled ferritin and aconitase IREs against both ferritin and aconitase probes, as well as the lack of competition by the unlabeled ferritin and aconitase mutant IREs bearing deletions of the first nucleotide from their respective IRE loops (ΔC fer, ΔC acon, Fig. 4*A*). Although aconitase and ferritin IRE probes of similar specific activities were used, complex formation was reproducibly stronger with the ferritin probe. This may reflect a lower affinity of the aconitase IRE for mammalian IRPs [as has also been observed for the eALAS IRE (20, 37)], or a greater sensitivity of aconitase IRE/IRP complexes to the experimental conditions. Similar results were obtained with extracts from murine B6 fibroblast cells (data not shown). In extracts prepared from cells that were pretreated for 8 h with heme arginate as an iron source, the iron chelator desferrioxamine or *S*-nitroso-*N*-acetyl-DL-penicillamine as an NO donor, or for 1 h with H_2O_2, the regulation of IRP binding to both IRE probes is clearly apparent (Fig. 4*B*, *upper*): it is augmented by iron deficiency (compare lanes 2 and 7 with lanes 3 and 8), H_2O_2 (compare lanes 4 and 9 with lanes 3 and 8), and NO (compare lanes 5 and 10 with lanes 3 and 8), and diminished in lysates from iron replete cells (compare lanes 1 and 6 with lanes 3 and 8). The similar IRE binding activities after addition of 2% 2-ME to the extracts (Fig. 4*B*, *lower*) indicates that the regulation in IRE binding occurs posttranslationally (29, 38). The composition of the complex with faster mobility (Fig. 4*B*, lanes 1–5) is not yet clearly defined. Competition experiments and the coregulation with IRP-1 suggest that the formation of this complex involves a specific IRE-binding protein (Fig. 4 and data not shown). Its apparent activation by 2-ME in lysates from control and iron replete cells argues against IRP-2 (3, 13), but would be consistent with the possibility that two complexes with different mobilities on native gels could be formed between IRP-1 and the aconitase IRE probe. This interpretation is also in line with the varying ratios between the faster and the slower migrating complexes in independent experiments performed with the same extract (compare Fig. 4*A*, lane 1 with Fig. 4*B*, lane 2). Nevertheless, our results confirm the specific binding of IRP-1 to the aconitase IREs. We conclude that this binding is regulated by the same three signals that control ferritin mRNA expression (K.P., G. Weiss, and M.W.H., unpublished work). The equal IRE binding by apo- and Fe-S IRP-1 reported earlier by Zheng *et al.* (21) apparently resulted from the inclusion of 50 mM DTT in their EMSA buffer with the

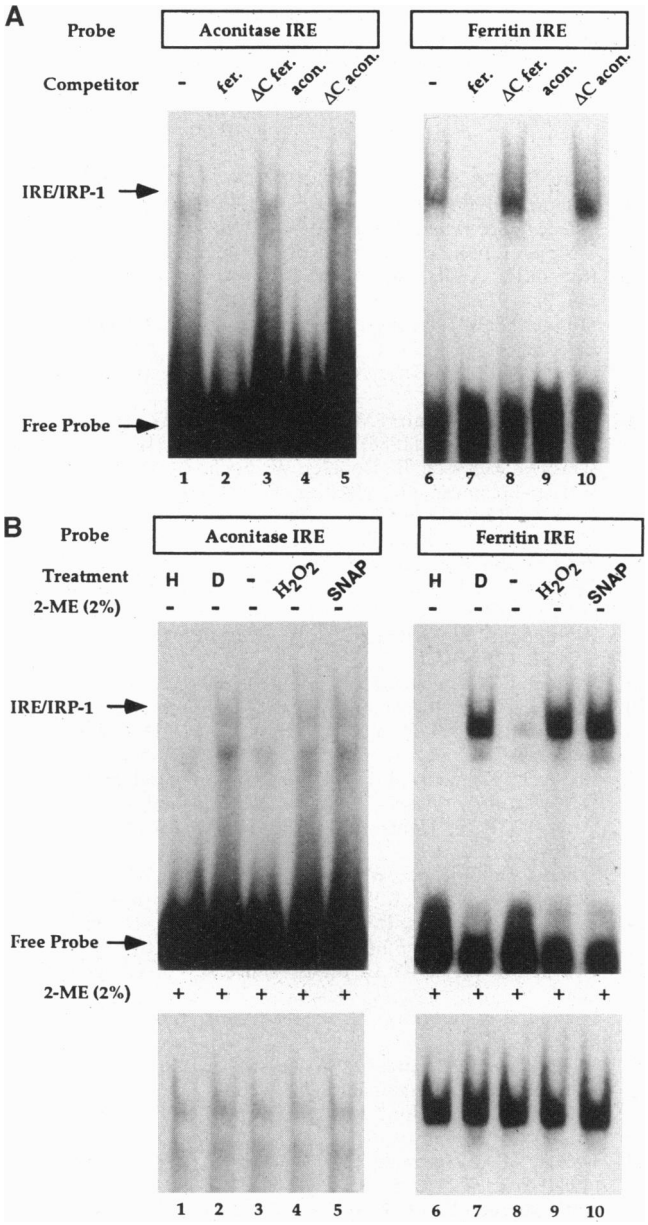

FIG. 4. Iron, NO, and H_2O_2-regulated specific binding of mammalian IRPs to the aconitase IRE. (*A*) Radiolabeled aconitase (lanes 1–5) or ferritin (lanes 6–10) IRE probes were incubated with 25 μg of extracts prepared from JB6 cells treated with 100 μM of desferrioxamine for 8 h. Unlabeled competitor RNAs (240 ng) containing either the ferritin H-chain IRE (fer; lanes 2 and 7), a mutant ferritin H-chain IRE (ΔC fer; lanes 3 and 8), the aconitase IRE (acon; lanes 4 and 9), or a mutant aconitase IRE competitor (ΔC.acon; lanes 5 and 10) were included as indicated. (*B*) Extracts from JB6 control cells (lanes 3 and 8) or cells pretreated with 100 μM of heme arginate (lanes 1 and 6), 100 μM of desferrioxamine (lanes 2 and 7), 100 μM of hydrogen peroxide (lanes 4 and 9), or 100 μM of *S*-nitroso-*N*-acetyl-DL-penicillamine (lanes 5 and 10) were incubated with the aconitase or ferritin IRE probe and analysed by EMSA. The autoradiographs in the left panels are exposed four to five times longer than those in the right panels.

purified protein which caused a similar *in vitro* activation of IRP-1 as we observe following the addition of 2-ME (Fig. 4*B*, *bottom*) (H. Beinert, personal communication).

The results obtained with the ferritin (5, 6, 8, 9), eALAS (7, 37), and the SDH-Ip IREs (Fig. 3) predict that the binding of IRP-1 to the aconitase IRE should repress the translation of the aconitase mRNA and that the regulation of this binding (Fig. 4*B*) should exert translational regulation. However, in contrast to the translational regulatory IREs in ferritin, eALAS and SDH-Ip mRNAs which are all located within the 5′ UTR (Fig. 1 *C*, *E*, and *F*), the aconitase IRE includes the translation initiation codon (Fig. 1 *A* and *B*). To test the function of IRP binding to an IRE including the initiator codon, we analyzed the authentic aconitase transcript rather than a reporter mRNA with the IRE inserted into the 5′ UTR. To allow an unambiguous assignment of IRP-imposed regulation to the IRE in this case, we also reconstructed the porcine aconitase mRNA with a point-mutated IRE (AcΔC) as a negative control. The result (Fig. 5*A*), including the internal U1A and external AcΔC controls, demonstrates the specific and IRE-dependent repression of porcine aconitase mRNA

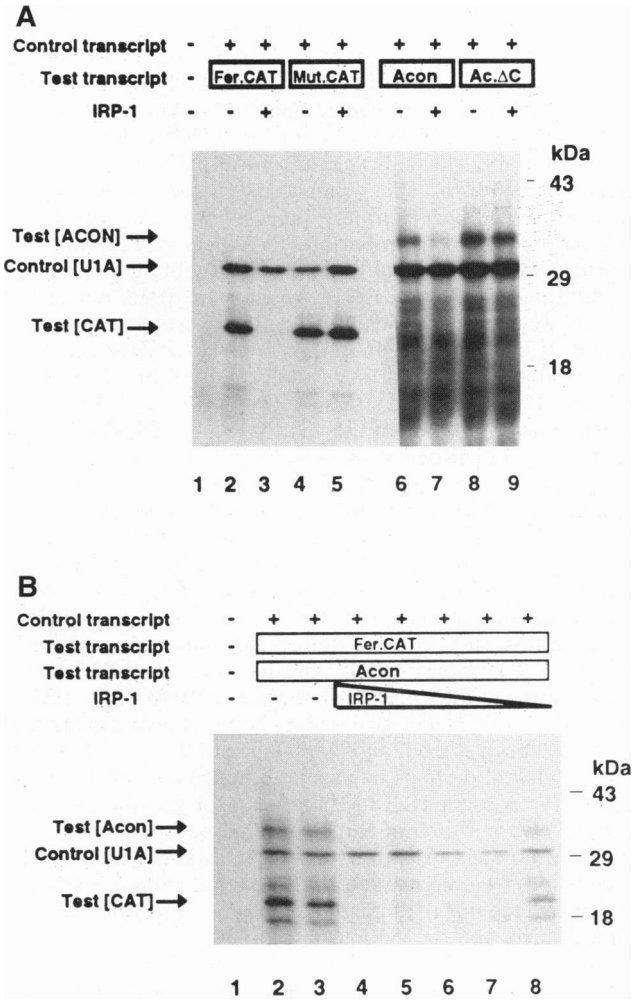

FIG. 5. Translational control of aconitase mRNA by IRP-1. (*A*) Capped U1A mRNA (2.5 ng) was cotranslated with 5 ng of capped Fer.CAT or Mut.CAT mRNAs or with 20 ng of capped Acon or Ac.ΔC mRNAs in wheat germ extract in the presence of IRP storage buffer (lanes 2, 4, 6, and 8) or 375 ng of recombinant human IRP-1 (lanes 3, 5, 7, and 9). (*B*) U1A (2.5 ng), Fer.CAT (5 ng), and Acon mRNAs (20 ng) were cotranslated in the presence of 500, 250, 125, 62.5, and 31.25 ng (lanes 4–8) of recombinant human IRP-1 or IRP storage buffer (lanes 2 and 3). No exogenous mRNA was added to the reactions shown in lane 1. Molecular weight markers are shown on the right and the positions of the U1A, CAT, and the C-terminally truncated aconitase protein products are shown on the left. The increased background from low molecular weight products in *A*, lanes 6–9 (cut off in *B*), originate from the inclusion of the Acon/Ac.ΔC mRNA (data not shown). At least in part, these low molecular weight polypeptides may be caused by the truncation of the aconitase open reading frame (39), which was necessary to avoid difficulties in the interpretation of the experiment arising from the limited ability of wheat germ extract to synthesize large proteins.

translation by recombinant IRP-1. To assess the relative regulatory capacity of the aconitase compared to the ferritin IRE, the Fer.CAT and Acon mRNAs were cotranslated in wheat germ extract (including U1A as an internal control) and titrated against recombinant IRP-1 (Fig. 5*B*). This direct comparison shows that the ferritin and the aconitase IREs display similar "functional affinities" for IRP-1, despite the weaker complex formation in EMSA (Fig. 4). Apparently, an IRE [which is positioned 13 nucleotides downstream from the cap structure (24)] can encompass the translation initiation codon of an mRNA with full function as a translational regulator.

The discovery of an IRE in the *D. melanogaster* SDH-Ip mRNA and the recognition of the conservation of an IRE in mitochondrial aconitase mRNA between two mammalian species prompted us to investigate the function of these elements. Taken together, the results demonstrate the role of both IREs as cis-acting mediators of IRP-regulated translation. We have thus identified a regulatory linkage between the control of iron homeostasis by the IRE/IRP system and the mitochondrial citric acid cycle, a central pathway for cellular energy metabolism. The strong conservation even between vertebrates and invertebrates suggests that this regulatory connection fulfills an important biological function(s). The approach taken in this study allowed us to obtain direct proof for the function of both IREs. At the same time, our results identify several questions for future investigations: Is the regulatory linkage between iron metabolism and the citric acid cycle of particular importance under certain metabolic conditions such as oxidative stress or iron deficiency? How is the translational regulation of the aconitase and SDH-Ip mRNAs functionally integrated with posttranslational modes for the regulation of the citric acid cycle enzymes (40–42)? Both cellular aconitases appear to be regulated in response to iron, NO, and H_2O_2 [the cytoplasmic aconitase (IRP-1) posttranslationally by means of its Fe-S cluster and the mitochondrial aconitase translationally by means of the IRE]. Is this coordinated regulation important for the control of the levels of the aconitase substrate citrate, an iron binding compound? Finally, no "consensus IRE" motifs were identified in the mammalian SDH-Ip mRNAs listed in release 44 of the EMBL database. Are *D. melanogaster* mitochondrial aconitase (which has not yet been cloned) and mammalian SDH-Ip mRNAs also IRE-regulated, perhaps by means of noncanonical IRP binding sites, or does the IRE-mediated control over the citric acid cycle involve a switch of target enzyme between vertebrates and invertebrates? Answers to these questions will yield new insights into what appears to have emerged from this study as an unexpected form of regulatory communication between mitochondria and the cytoplasm.

We thank Dr. Howard Zalkin for the porcine mitochondrial aconitase cDNA, Dr. Immo Scheffler for the *D. melanogaster* SDH-Ip cDNA, Dr. Klaus Schulze-Osthoff for the JB6 cell line, and Dr. Lisbeth Olson for her kind gift of *D. melanogaster* embryo extracts. Heme arginate was a kind gift from Leiras Oy (Finland). B.A.C.A. was supported by National Institutes of Health Grant HL-16251, N.K.G. and K.P. are funded by a grant from the Deutsche Forschungsgemeinschaft to M.W.H.

1. Melefors, Ö. & Hentze, M. W. (1993) *BioEssays* **15,** 85–90.
2. Klausner, R. D., Rouault, T. & Harford, J. B. (1993) *Cell* **72,** 19–28.
3. Guo, B., Yu, Y. & Leibold, E. A. (1995) *J. Biol. Chem.* **269,** 24252–24260.
4. DeRusso, P. A., Philpott, C. C., Iwai, K., Mostowski, H. S., Klausner, R. D. & Rouault, T. A. (1995) *J. Biol. Chem.* **270,** 15451–15454.
5. Swenson, G. R., Patino, M. M., Beck, M. M., Gaffield, L. & Walden, W. E. (1991) *Biol. Metals* **4,** 48–55.
6. Walden, W. E., Patino, M. M. & Gaffield, L. (1989) *J. Biol. Chem.* **264,** 13765–13769.
7. Melefors, Ö., Goossen, B., Johansson, H. E., Stripecke, R., Gray, N. K. & Hentze, M. W. (1993) *J. Biol. Chem.* **268,** 5974–5978.
8. Gray, N. K., Quick, S., Goossen, B., Constable, A., Hirling, H., Kühn, L. C. & Hentze, M. W. (1993) *Eur. J. Biochem.* **218,** 657–667.
9. Gray, N. K. & Hentze, M. W. (1994) *EMBO J.* **13,** 3882–3891.
10. Binder, R., Horowitz, J. A., Basilion, J. P., Koeller, D. M., Klausner, R. D. & Harford, J. B. (1994) *EMBO J.* **13,** 1969–1980.
11. Casey, J. L., Hentze, M. W., Koeller, D. M., Caughman, S. W., Rouault, T. A., Klausner, R. D. & Harford, J. B. (1988) *Science* **240,** 924–928.
12. Müllner, E. W., Neupert, B. & Kühn, L. C. (1989) *Cell* **58,** 373–382.
13. Henderson, B. R., Seiser, C. & Kühn, L. C. (1993) *J. Biol. Chem.* **268,** 27327–27334.
14. Rouault, T. A., Hentze, M. W., Caughman, S. W., Harford, J. B. & Klausner, R. D. (1988) *Science* **241,** 1207–1210.
15. Weiss, G., Goossen, B., Doppler, W., Fuchs, D., Pantopoulos, K., Werner-Felmayer, G., Wachter, H. & Hentze, M. W. (1993) *EMBO J.* **12,** 3651–3657.
16. Martins, E. A. L., Robalinho, R. L. & Meneghini, R. (1995) *Arch. Biochem. Biophys.* **316,** 128–134.
17. Drapier, J. C., Hirling, H., Wietzerbin, J., Kaldy, P. & Kühn, L. C. (1993) *EMBO J.* **12,** 3643–3649.
18. Pantopoulos, K. & Hentze, M. W. (1995) *Proc. Natl. Acad. Sci. USA* **92,** 1267–1271.
19. Pantopoulos, K. & Hentze, M. W. (1995) *EMBO J.* **14,** 2917–2924.
20. Dandekar, T., Stripecke, R., Gray, N. K., Goossen, B., Constable, A., Johansson, H. E. & Hentze, M. W. (1991) *EMBO J.* **10,** 1903–1909.
21. Zheng, L., Kennedy, M. C., Blondin, G. A., Beinert, H. & Zalkin, H. (1992) *Arch. Biochem. Biophys.* **299,** 356–360.
22. Stripecke, R. & Hentze, M. W. (1992) *Nucleic Acids Res.* **20,** 5555–5564.
23. Scherly, D., Boelens, W., van Venrooij, W. J., Dathan, N. A., Hamm, J. & Mattaj, I. W. (1989) *EMBO J.* **8,** 4163–4170.
24. Zheng, L., Andrews, P. C., Hermodson, M. A., Dixon, J. E. & Zalkin, H. (1990) *J. Biol. Chem.* **265,** 2814–2821.
25. Gray, N. K. (1994) Ph.D. thesis (University of Glasgow, Scotland).
26. Leibold, E. A. & Munro, H. N. (1988) *Proc. Natl. Acad. Sci. USA* **85,** 2171–2175.
27. Dandekar, T. & Hentze, M. W. (1995) *Trends Genet.* **11,** 45–50.
28. Hentze, M. W., Caughman, S. W., Casey, J. L., Koeller, D. M., Rouault, T. A., Harford, J. B. & Klausner, R. D. (1988) *Gene* **72,** 201–208.
29. Hentze, M. W., Rouault, T. A., Harford, J. B. & Klausner, R. D. (1989) *Science* **244,** 357–359.
30. Rothenberger, S., Müllner, E. W. & Kühn, L. C. (1990) *Nucleic Acids Res.* **18,** 1175–1179.
31. Haile, D. J., Rouault, T. A., Tang, C. K., Chin, J., Harford, J. B. & Klausner, R. D. (1992) *Proc. Natl. Acad. Sci. USA* **89,** 7536–7540.
32. Constable, A., Quick, S., Gray, N. K. & Hentze, M. W. (1992) *Proc. Natl. Acad. Sci. USA* **89,** 4554–4558.
33. Au, H. C. & Scheffler, I. E. (1994) *Gene* **149,** 261–265.
34. Goossen, B., Caughman, S. W., Harford, J. B., Klausner, R. D. & Hentze, M. W. (1990) *EMBO J.* **9,** 4127–4133.
35. Goossen, B. & Hentze, M. W. (1992) *Mol. Cell. Biol.* **12,** 1959–1966.
36. Dunkov, B. C., Zhang, D., Choumarov, K., Winzerling, J. J. & Law, J. H. (1995) *Arch. Insect Biochem. Physiol.* **29,** 293–307.
37. Bhasker, C. R., Burgiel, G., Neupert, B., Emery-Goodman, A., Kühn, L. C. & May, B. K. (1993) *J. Biol. Chem.* **268,** 12699–12705.
38. Pantopoulos, K., Gray, N. K. & Hentze, M. W. (1995) *RNA* **1,** 155–163.
39. Minshull, J. & Hunt, T. (1992) in *Antisense RNA and DNA*, ed. Murray, J. A. H. (Wiley–Liss, New York), Vol. 11, pp. 195–212.
40. Gardner, P. R., Nguyen, D.-D. & White, C. W. (1994) *Proc. Natl. Acad. Sci. USA* **91,** 12248–12252.
41. Hausladen, A. & Fridovich, I. (1994) *J. Biol. Chem.* **269,** 29405–29408.
42. Castro, L., Rodriguez, M. & Radi, R. (1994) *J. Biol. Chem.* **269,** 29409–29415.